

ARTICLE OPEN



Multifunctional biomimetic tactile system via a stick-slip sensing strategy for human–machine interactions

Yue Li^{1,2}, Manjun Zhao³, Yadong Yan⁴, Luanxi He³, Yingyi Wang⁵, Zuoping Xiong^{1,2}, Shuqi Wang², Yuanyuan Bai², Fuqin Sun², Qifeng Lu⁵, Yu Wang⁴, Tie Li^{1,2,6} and Ting Zhang^{1,2,6,7}

A tactile sensor system enables natural interaction between humans and machines; this interaction is crucial for dexterous robotic hands, interactive entertainment, and other smart scenarios. However, the lack of sliding friction detection significantly limits the accuracy and scope of interactions due to the absence of sophisticated information, such as slippage, material and roughness of held objects. Here, inspired by the stick-slip phenomena in the sliding process, we have developed a multifunctional biomimetic tactile system based on the stick-slip sensing strategy, which is a universal method to detect slippage and estimate the surface properties of objects by sliding. This system consists of a flexible fingertip-inspired tactile sensor, a read-out circuit and a machine-learning module. Based on the stick-slip sensing strategy, our system was endowed with high recognition rates for slippage detection (100.0%), material classification (93.3%) and roughness discrimination (92.8%). Moreover, robotic hand manipulation, interactive games and object classification are demonstrated with this multifunctional system for comprehensive and promising human–machine interactions.

npj Flexible Electronics (2022)6:46; <https://doi.org/10.1038/s41528-022-00183-7>

INTRODUCTION

Human–machine interaction (HMI) systems with tactile sensors can provide precise input signals and the required feedback between users and machines; such systems are increasingly requested for the aspects of advanced robots^{1–3}, smart homes^{4,5}, interactive entertainment^{6,7} and health care^{8,9}. Compared with traditional interaction approaches, such as keyboards, mouse and touch panels, various emerging HMIs possessing flexible tactile sensors have been proposed for conformal contact with human skin to achieve a natural interaction experience. These HMIs include smart gloves for virtual reality and augmented reality^{7,10}, arm sleeves for hand motion detection^{11,12}, and smart textiles for health care^{13,14}. In these systems, tactile sensors are essential for obtaining signals from the external environment; these signals are still insufficient for research on multiple mechanical sensing techniques. Therefore, there is an urgent need for the development of advanced tactile sensors and derived systems to push the boundaries of HMI applications.

Recently, various tactile sensors have been developed based on piezoresistive^{15,16}, piezoelectrical^{17,18}, capacitive^{19,20}, triboelectric mechanisms^{21,22}, and they mainly focus on the normal force in terms of mechanical sensing. However, the detection of sliding friction force is easily neglected and not advanced enough due to the lack of understanding of the interfacial slippage. Normal force sensing is related to touch, and sliding friction sensing is closely related to slippage detection, material classification and roughness recognition by sliding. Until recently, sliding friction force has mainly been detected by sensor arrays through changes in pressure mapping to judge the displacement of an object, but only if the object partially slipped off sensor arrays or the size of

objects was smaller than that of sensor arrays^{23–25}; these constraints limit the universal application of sliding friction force in haptic interactions. In contrast, the sensory system of humans can sense slippage precisely²⁶ and discern different objects, such as velvet, from wool reliably by sliding fingertips on the surface²⁷, which benefits from the sophisticated structure of fingertips²⁸. To date, there is no such artificial tactile sensor to achieve the above functions. Therefore, for the more natural and functional haptic interactions of HMI, there is an urgent demand to develop a specific strategy to sensitively measure normal force, precisely detect slippage, discriminate material and recognize roughness similar to humans.

The stick-slip phenomenon is enlightening for monitoring slippage and detecting abundant information related to sliding friction. According to the theory of tribology, dry friction is a spontaneous jerking motion, rather than a continuous and stationary motion, which occurs while two objects slide over each other, which is called the stick-slip phenomenon^{29,30}. We found that the above stick-slip phenomenon also occurred on the flexible tactile sensor when sliding on the surface of an object, resulting in the fluctuation of sensor signals. In addition, the fluctuations are also different during sliding on different objects. Hence, the existence of signal fluctuations is used as a judgment criterion for the occurrence of slippage, and the differences of signal fluctuations are used for material classification and roughness discrimination, which are concluded as the stick-slip sensing strategy and employed for our multifunction tactile system.

Under the above stick-slip sensing strategy, we set up a multifunction machine-learning-assisted tactile system for HMIs with the abilities of force sensing, slippage detection, material

¹School of Nano-Tech and Nano-Bionics, University of Science and Technology of China, Hefei, Anhui, PR China. ²i-Lab, Nano-X Vacuum Interconnected Workstation, Key Laboratory of Multifunction Nanomaterials and Smart Systems, Suzhou Institute of Nano-Tech and Nano-Bionics (SINANO), Chinese Academy of Sciences (CAS), Suzhou, PR China. ³School of Electronic Science and Engineering, University of Electronic Science and Technology of China, Chengdu, PR China. ⁴School of Biological Science and Medical Engineering, Beihang University, Beijing, PR China. ⁵Department of Health and Environmental Sciences, School of Chips, XJTLU Entrepreneur College (Taicang), Xi'an Jiaotong-Liverpool University, Suzhou, Jiangsu, PR China. ⁶Gusu Laboratory of Materials Science, Suzhou, PR China. ⁷Center for Excellence in Brain Science and Intelligence Technology, Chinese Academy of Science, Shanghai, PR China. ✉email: tli2014@sinano.ac.cn; tzhang2009@sinano.ac.cn

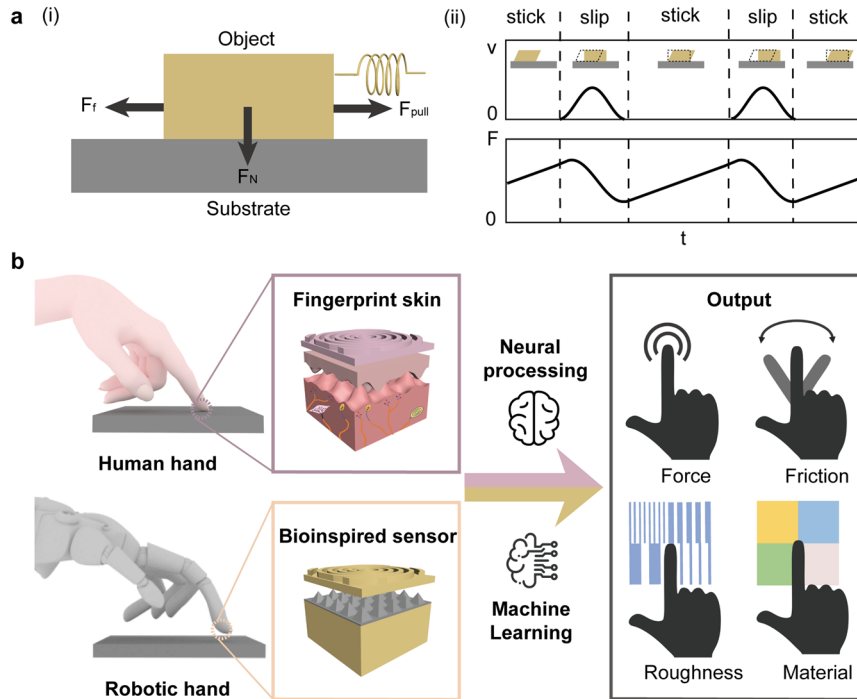


Fig. 1 Schematic illustrations of the stick-slip sensing strategy and the fingertip-inspired multifunction tactile sensor system. **a** (i) Simple frictional system contains an object that connected to a spring sitting on a frictional surface. The force F_{pull} is set to keep the object moving given a normal force F_N . F_f is a force resisting the relative motion of object sliding against each other, which opposes the relative lateral motion of two solid surfaces in contact. (ii) The sliding friction force and speed as a function of time. According to the simple friction system, the force in the spring will increase with time until the force is sufficient to overcome the static frictional force. If the object then moves forward suddenly at a velocity greater than the velocity of the spring move, the force in the spring will decrease and the object will eventually stop. The object will remain stationary until the force in the spring once more builds up to a value sufficient to overcome the static frictional force. **b** Schematic illustration of the multifunction tactile system, containing the bionic design of tactile sensor, signals processing and output information, possessing the ability of force sensing, slippage detection, material classification and roughness discrimination.

classification and roughness discrimination. Inspired by the human tactile perception system, this multifunction tactile system consists of a fingertip-inspired tactile sensor, a read-out circuit and a set of machine-learning algorithms. The fingertip-inspired sensor contains an epidermis-inspired double-helix top layer and a spinosum-inspired pyramidal bottom layer, which are designed for transmitting vibrations obtained from stick-slip phenomena and sensibilization, respectively. With the aid of the algorithm, the system has a high recognition rate of 100.0% for static and sliding statuses and possesses the ability to discriminate the six types of materials (93.3%) and six different roughnesses (92.8%). Furthermore, we set up proof-of-concept applications of this multifunctional system to demonstrate the potential prospects in HMI.

RESULTS

The stick-slip phenomenon of interfacial slippage

The model and mathematical description of the stick-slip phenomenon are presented in Fig. 1a, which is helpful for the design of a multifunctional tactile system to monitor slippage and detect abundant information. In daily life, there are many common examples that produce vibrations due to stick-slip friction, for example, rubbing chalk on a blackboard and brakes screeched as the car stops. As a general and important phenomenon, stick slip can be described as surfaces alternating between sticking to each other and sliding over each other, with a corresponding change in the force of friction³¹. Typically, the static friction coefficient (a heuristic number) between two surfaces is larger than kinetic one. If a small drawing force is applied to an object, it remains stationary on a rough surface owing to the presence of static frictional force, corresponding to a velocity of

zero. As the drawing force increases to larger than the static frictional force, the object starts to move, corresponding to a jump in the velocity. This jerking motion is illustrated in Fig. 1a and the following formulas (1) and (2),

$$t_{slip} = \frac{2}{\omega} \arctan\left(\frac{\omega F_s - F_k}{v_0 c}\right) \quad (1)$$

where t_{slip} is the duration of the stick phase, ω is the angular velocity, v_0 is the constant velocity, F_s is the static friction force, F_k is the kinetic friction force and c is a constant.

$$\Delta x_{slip} = 2 \frac{F_s - F_k}{c} \quad (2)$$

where Δx_{slip} is the sliding length, F_s is the static friction force, F_k is the kinetic friction force and c is a constant. Detailed theoretical analysis and formula deduction are presented in Supplementary Note³². F_s and F_k depend upon the combined effects of material deformation characteristics and surface roughness, both of which have their origins in the chemical bonding at the contact surface^{33,34}. Accordingly, the stick-slip phenomenon can also provide information about the mechanical properties of the surface (e.g., friction, surface roughness, material characteristics, etc.)

Fabrication and characterization of sensors

The measurement of the stick-slip phenomenon is closely related to the design of flexible tactile sensors. A fingertip is the ideal bionic prototype that has the ability to sense force and vibration due to stick slip. On the microscopic scale, the moving fingertip and the touched object form a frictional system, which researchers have long known to generate jerky stick-slip movement^{35–37}.

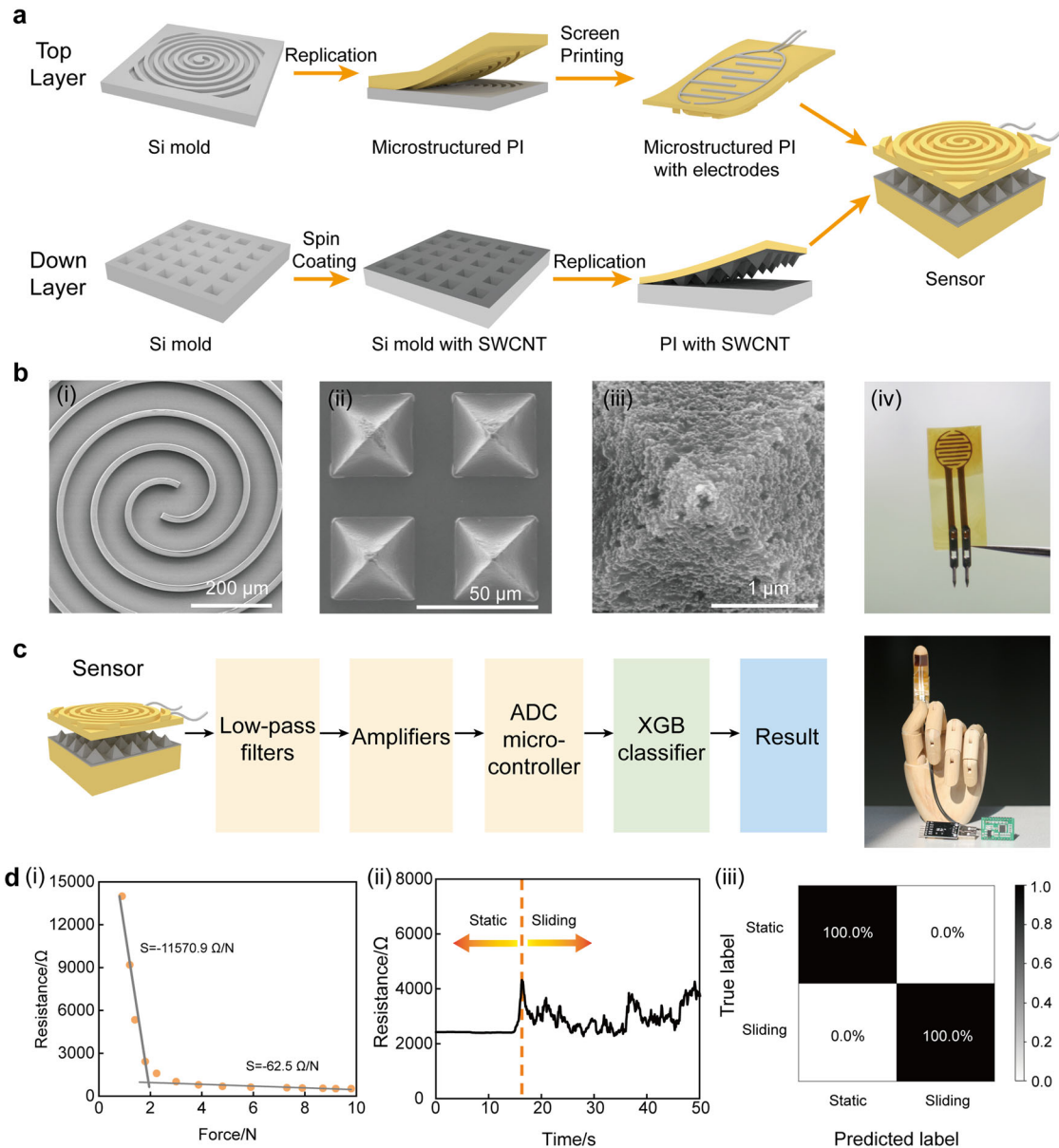


Fig. 2 The fabrication, characterization and performance of the tactile sensor. **a** A schematic illustration of the fingertip-inspired sensor fabrication process. **b** Scanning electron microscopy (SEM) images and optical image of the sensor. (i) the top fingertip-inspired layer. (ii) the down micropyramid layer. (iii) the single carbon nanotube partially embedded in the patterned surface. (iv) the optical image of the sensor. **c** The integration of the multifunction tactile system, showing analog signal acquisition, processing (orange) and machine-learning recognition (green) paths from the sensor to the custom-developed peripherals. **d** output signals of static and sliding status. (i) responses of the tactile sensor under different normal force. (ii) real-time responses of the sensor from static to sliding state with a constant normal force (2 N) and a constant sliding velocity (100 mm min^{-1}). (iii) The confusion matrix derived from the model made by XGBoost. Predicted label refers to the recognized results, and true label refers to the true state. The color bar represents the normalized accuracy.

Besides, the fingertip contains dermis, epidermis and subcutaneous tissue²⁷, as shown in Fig. 1b. Fingerprints are ridges on the epidermis, which is closely related to exquisite tactile sensitivity^{38,39}. The spinosum is a layer between the dermis and the epidermis, forming interlocked microstructures responsible for tactile signal amplification. In the subcutaneous tissue, four types of mechanoreceptors (Meissner corpuscles, Merkel cells, Ruffini endings, and Pacinian corpuscles) are distributed with a high density in particular and are selectively sensitive to dynamic skin deformation, static force, vibration or applied stretching of the skin²⁸. Due to the stick-slip movement, different regions of the contact area were subject to varying degrees of compression, stretch and shear. And tactile mechanoreceptors of different

regions will produce action potentials discontinuously in space and time, which are conveyed to the brain to generate perception⁴⁰.

Inspired by the above sensing mechanism of fingertips, a bionic flexible tactile sensor containing a epidermis-inspired double-helix layer and a spinosum-inspired pyramidal layer was designed, as depicted in Fig. 1a. Polyimide was chosen as the substrate material due to its mechanical and wearproof properties. For the epidermis-inspired layer, a double-helix structure was built to mimic the ridges on the epidermis through the replication process, as shown in the scanning electron microscopy image of Fig. 2b-i. The double-helix structure is centrosymmetric, which ensures the constant sensitivity to sliding from any direction in

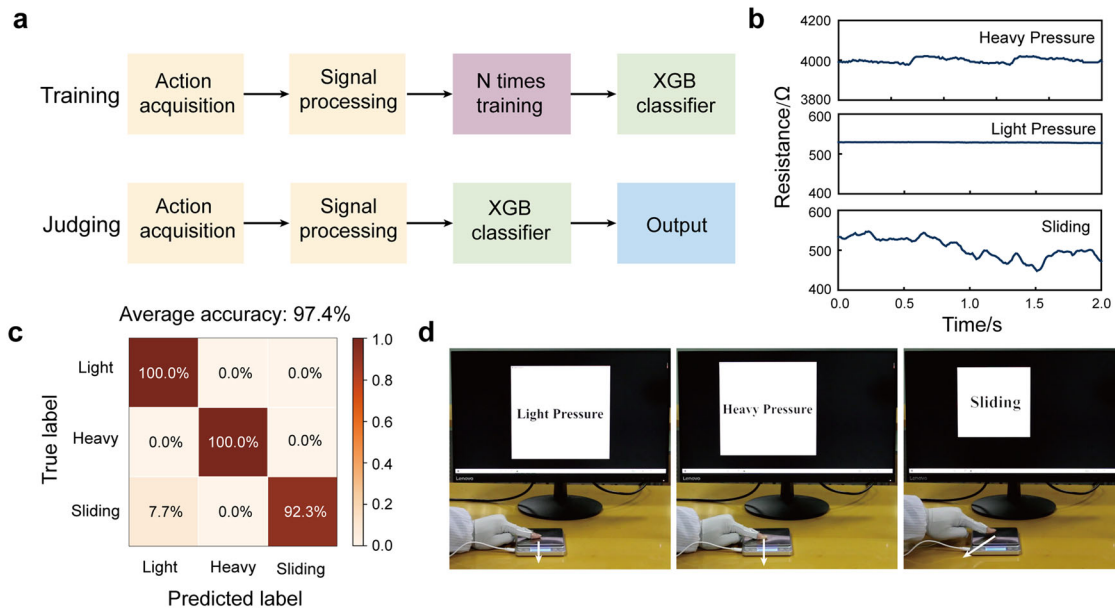


Fig. 3 Demonstration of the multifunction tactile system for the discrimination of light, heavy pressure and slippage. **a** Machine-learning-assisted data process flow, including a training process and an actual judging process. **b** A set of typical signals of the bioinspired sensor equipped on the human finger corresponding to light, heavy pressure and slippage. **c** Confusion matrix of classification test derived from the model made by XGBoost. Predicted label refers to the recognized results, and true label refers to the true status. The color bar represents the normalized accuracy. **d** Photographs of the actual online judging demonstration of human hand integrated with the bioinspired sensor for light, heavy pressure and slippage recognition. The recognition results were shown in the screen. The arrows represent the direction of applied force.

plane (Supplementary Fig. 2). Then, silver electrodes were printed on the other side of the top fingerprint layer by screen printing. For spinosum-inspired layer, micropylamids were employed to improve the sensitivity, and single-wall carbon nanotubes (SWCNTs) were chosen as the sensing material due to their electrical conductivity. Through spray-coating and replicating processes, the micropylamid layer was demoulded easily (Fig. 2b-ii) with partially embedded SWCNTs on the surface (Fig. 2b-iii), which gives high stability to avoid contact-induced degradation and good conductivity.

The stick-slip sensing strategy

According to the resistance value of the above fingertip-inspired sensor, multifunctional information can be detected, including pressure, slippage, material and roughness. Normal force sensing relies on the modulation of contact resistance via applied pressure, which is caused by a change in contact area between a conductor and an electrode. Fig. 2d shows the response of the sensor in the pressure range of 0–10 N, and the sensitivities are estimated from the slopes of the linear fits as $-11570.9 \Omega \text{ N}^{-1}$ for 0–1.8 N ($R^2 = 0.92$) and $-62.5 \Omega \text{ N}^{-1}$ for 3–10 N ($R^2 = 0.77$), respectively.

Slippage detection is based on the stick-slip phenomenon when two objects slide over each other. During the sliding status, the force (F_{pull}) was applied to set the system in motion. However, elasticity, inherent in all objects, reduces the effective driving force by temporarily storing some of the applied energy into the elastic deformation of objects. By doing so, the effective driving force may drop below the requirement for keeping the system in motion, and it comes to a momentary standstill, only to be followed by a further jump forward once the accumulating elastic force together with the externally applied force exceed friction again. This stick-slip phenomenon could affect the contact area between a conductor and an electrode, resulting in the fluctuation of resistance of the fingertip-inspired sensor, which is the criterion for slippage.

The fluctuation of resistance caused by the stick-slip phenomenon during the sliding process is affected by material characteristics and surface roughness. For material characteristics, the stronger viscosity due to the van der Waals force retains a higher resistance to motion when sliding in the kinetic state. Higher elasticity can better conform to the contact surface and form less contact movement, leading to remarkable stick-slip effects. In addition, surface roughness also influences the fluctuation frequency of the stick-slip phenomenon, and the surface microstructure of sensors at the contact surface can enhance this fluctuation. According to the difference of fluctuations when sliding on the visous material and roughness surface, this multifunction sensor-based tactile system has the ability to material classification and roughness discrimination with the assistance of the machine-learning algorithm.

The integration of the multifunction tactile system

With the above fingertip-inspired sensor, a multifunction sensing system was set up, which consists of a fingertip-inspired sensor, a read-out circuit and a machine-learning module. Fig. 2c provides the flow chart of both hardware and software, beginning with analogue signal acquisition, then conditioning and processing, and finally wire transmission to the computer, which is embedded with a machine-learning algorithm for robust detection. For the hardware of analogue signal acquisition and processing, Keithley 2602 was used to measure the resistance of the sensor, and a printed circuit board (PCB) was designed for the HMI in view of portability. The PCB realizes multiple functions of signal conditioning, processing and transmission via available integrated circuit components, as depicted in Supplementary Fig. 1. Since the characteristic of stick-slip movement is an empirical measurement and cannot be found through calculations, a machine-learning algorithm was chosen to classify the processed signals rather than the traditional logic circuit judgment designed according to a truth table. To our knowledge, this emerging machine-learning tool is effective at distilling information, and many classes of

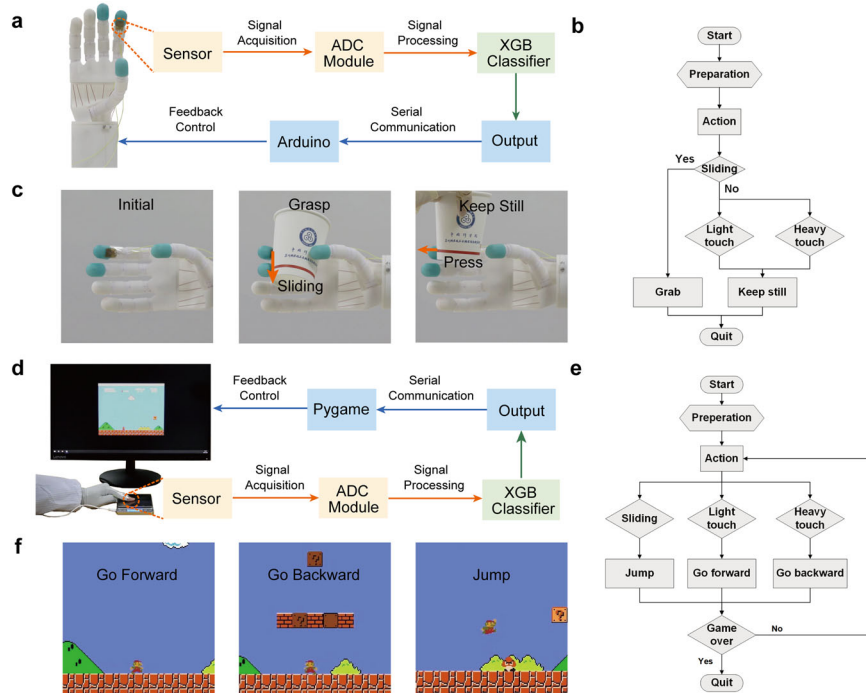


Fig. 4 Close-loop control of robotic hand and interactive Super Mario game assisted with the multifunction tactile system. **a** Schematic illustrations for the robotic hand assisted with the multifunction tactile system, containing analog signal acquisition, processing, machine-learning recognition, feedback control of robotic hand through Arduino. **b** Flow chart for the grasp operation of robotic hands. **c** Photographs of actual online feedback control in response to the slippage and touch of a cup. (i) initial state, (ii) grasp once the slippage occur, (iii) keep still when only measured light or heavy touch. **d** Schematic illustrations for the interactive Super Mario game assisted with the multifunction tactile system, showing the human finger equipped with the bioinspired sensor, analog signal acquisition, processing, machine-learning recognition, interactive events in Super Mario through pygame. **e** Flow chart for the operation of Super Mario game. **f** Screenshots of actual online interactive Super Mario game in response to the light touch, heavy touch and slippage by index finger, (i) go forward if light touch occur, (ii) go backward once heavy touch occur, (iii) jump if sliding happen.

algorithms can be readily used with tactile data. Considering the single signal of the sensor and the complexity of the algorithm, XGBoost was adopted, which is an optimized distributed gradient boosting library. It can provide parallel tree boosting that solves many data problems in a fast and accurate way by implementing the algorithms under the Gradient Boosting framework. The classifier can be obtained through XGBoost training and then send output signals to control the external machine to complete the feedback control.

The systematic demonstration of slippage detection for HMI

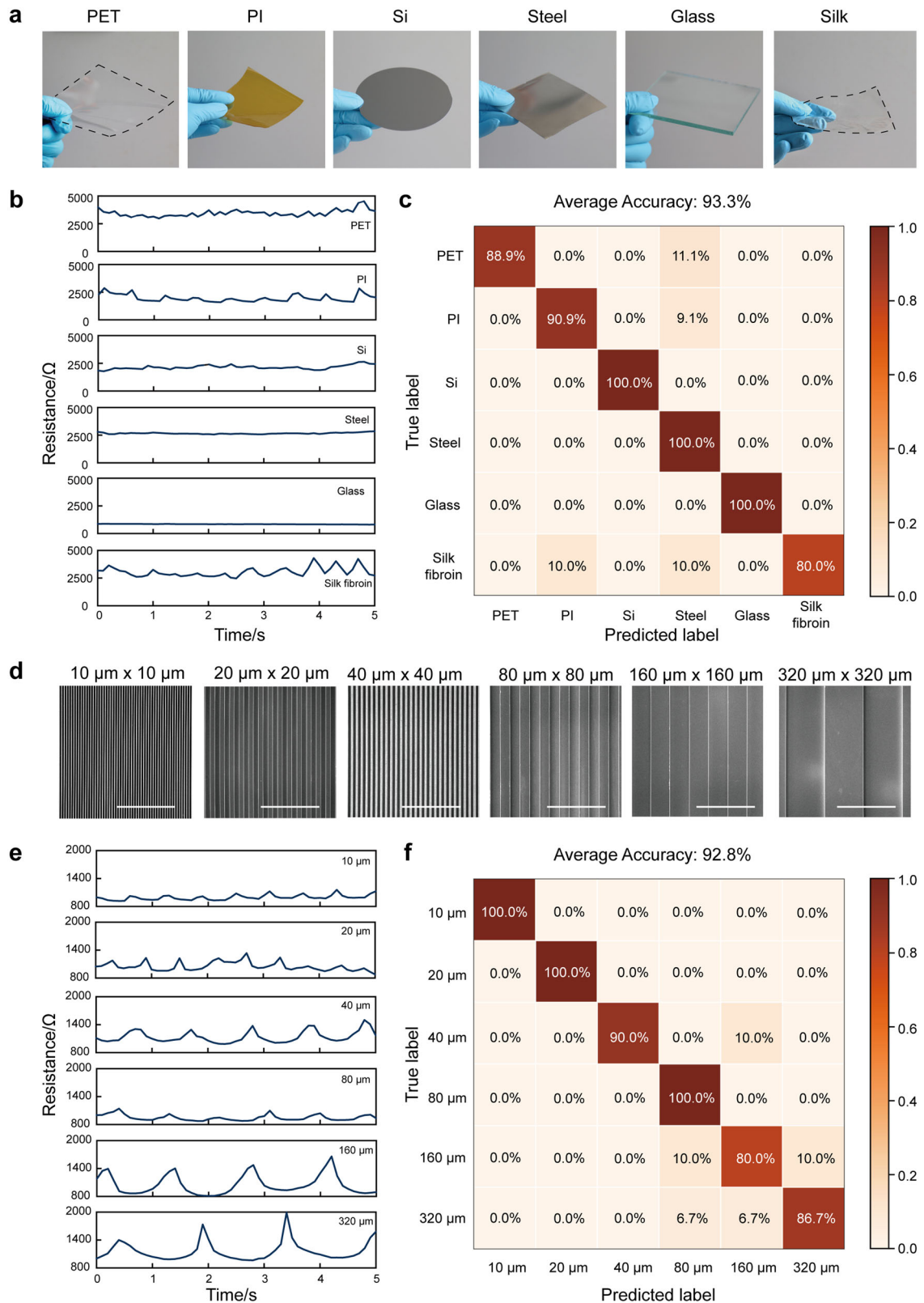
Slippage detection broadens the tactile information of HMI, except pressure sensing. For this multifunction sensing system, the sensory signals were classified by the machine-learning algorithm, which can effectively improve the accuracy and robustness of the classification. A flow diagram of the machine-learning process is shown in Fig. 3a, which includes training and a subsequent actual judging process.

With the above multifunctional sensing system via a stick-slipping sensing strategy, we have demonstrated the remarkable ability of slippage recognition. The response of this fingertip-inspired sensor was tested under static and sliding conditions on a polyethylene terephthalate (PET) film. The friction coefficient apparatus was used to execute controllable and repeatable sliding with a constant normal force of 2 N under a speed of 100 mm min^{-1} (Supplementary Fig. 3). As shown in Fig. 2d, the resistance of this sensor remained unchanged in the static state and had a relatively large fluctuation in the sliding state, which is consistent with the theoretical prediction. Then, to accomplish the training process, these static and sliding actions were repeated 50 times and continued for 20 s each time, and the corresponding electrical

signals were measured by a Keithley 2602 with a sampling frequency of 10 Hz. Here, the obtained 50 data samples of each status are used for training (80%) and testing (20%) and labeled according to classes. After training by XGBoost, the accuracy for static and sliding recognition reached 100.0%, as depicted in the confusion matrix (Fig. 2d).

Apart from the ability to recognize slippage, this system also has the basic ability of sensing force. As shown in Fig. 3d, the fingertip-inspired sensor was mounted on the finger to perform three different actions, including sliding and heavy and light touch. During the training process, each class of action was repeated 50 times and lasted for 2 s per session. The corresponding electrical signals were measured by PCB with a sampling frequency of 100 Hz and labeled according to classes. Based on the labeled database, the XGBoost model was then generated. Specifically, 50 data samples of each gesture are obtained for training (80%) and testing (20%). After training, the average accuracy of the XGBoost model for action recognition reached 97.4%, as depicted in Fig. 3c. During the judging process, a random action was performed and measured by PCB. Subsequently, the XGBoost model was used to classify the action. As shown in Fig. 3d and Supplementary Movie 1, the actual actions were classified online with high accuracy, demonstrating that the multifunction tactile system has the ability to recognize and classify light touch, heavy touch and sliding effectively.

In addition to multifunction sensing, we also employed the output of this multifunction tactile system to control the external tendon-driven soft robotic hand to perform a closed-loop sensing control system, as shown in Fig. 4a. The continuum structure was used as the finger joint. The other four fingers except the middle finger can perform flexion/extension and abduction/adduction



movements, which benefits hand mobility. In the demonstration, the index finger of the robotic hand was equipped with the fingertip-inspired tactile sensor ahead. For the sensing of the robotic hand, the electrical signals, which were closely related to the force and slippage, were processed with analogue-to-digital

conversion, conditioning and processing. Then, the analogue signal was transferred to the XGBoost classifier model, which was trained in advance. Next, for the feedback of the robotic hand, the Arduino, which is an open-source electronic prototyping platform, monitored the judgment of the XGBoost classifier model in real

Fig. 5 The ability of the multifunction tactile system for material classification and roughness discrimination. **a** Photographs of six different objects with various materials and similar roughness, containing PET film, PI film, silicon wafer, stainless steel sheet, glass and silk film. **b** Details of the corresponding responses of the bioinspired sensor during sliding on above objects with the constant normal force of 2 N and sliding velocity of 100 mm min^{-1} . **c** Confusion matrix of materials discrimination from the model trained by XGBoost. Predicted label refers to the recognized results, and true label refers to the true materials. **d** SEM images of six different silicon wafers with various roughness with the same depth ($40 \mu\text{m}$) and six kinds of spacing and width. Scale bar represents $500 \mu\text{m}$. **e** Details of the corresponding responses of the bioinspired sensor during sliding on above silicon wafers with the constant normal force of 2 N and sliding velocity of 100 mm min^{-1} . **f** Confusion matrix of roughness discrimination from the model made XGBoost. Predicted label refers to the recognized results, and true label refers to the true roughness. The color bar represents the normalized accuracy.

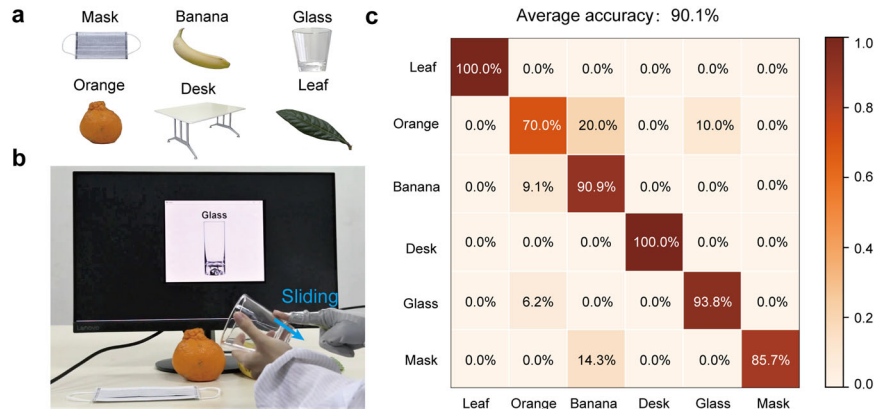


Fig. 6 Demonstration of the multifunction tactile system for objects recognition. **a** photographs of six objects containing mask, banana, glass, orange, desk and leaf. **b** The actual online recognition by dragging the bioinspired sensor on the target object and then the recognition result showed on the screen. The blue arrow identified the direction of sliding. **c** Confusion matrix of above six objects recognition from the model trained by XGBoost. Predicted label refers to the recognized results, and true label refers to the true objects. The color bar represents the normalized accuracy.

time and finally controlled the linear servo motors of robotic fingers according to this judgment (Supplementary Fig. 4). With this multifunctional tactile sensing system, the robotic hand has the ability to sense light touch, heavy touch and slippage and then provides corresponding feedback for dexterous manipulation. This overall closed-loop process is summarized in the flow chart of Fig. 4b. The actual online demonstration is displayed in Fig. 4c and Supplementary Movie 2. The robotic hand will grasp the cup gently once the finger ‘feels’ the slippage of the cup, and it will keep the initial state if “feeling” light or heavy touch.

In addition to the closed-loop control of robotic hands, an interactive game was also set up based on the multifunction sensing system, in which humans can perform specific actions to play the Super Mario game by wearing the sensor on the fingertip (Fig. 4d). A Super Mario game was written by a Pygame module with flow control, animated graphs, collision detection and so on. According to the flow chart of the interaction process in Fig. 4e, the electrical signal was measured, and then the XGBoost classifier output the judgment to control the movement of Mario. As demonstrated by the actual online interactive game shown in Fig. 4f and Supplementary Movie 3, actions of the index finger, including light touch, heavy touch and sliding, can keep Mario go ahead, go back and jump, respectively. With this function, this multifunctional tactile system has the potential to enrich the modes of HMI.

Material classification and roughness discrimination

In addition, this multifunctional sensing system can distinguish materials and roughness. To our knowledge, previous studies have mainly focused on material discrimination through high-density pressure mapping. Particularly, in regard to material discrimination, such as the intrinsic properties of inter-surface adhesion and surface deformation, studies are still lacking. However, the more

detailed the information the HMI system obtains, the more accurate the interaction is.

According to the theory of tribology, the stick-slip movement at the interface is determined by F_S and F_K , which are closely related to the properties of the materials and roughness. For material distinction, six different samples with the same roughness were obtained (Fig. 5a), containing silicon slices, polyimide films, PET films, silk films, glass and steel; their actual surface roughness morphologies are shown in Supplementary Fig. 5. During the training process, sliding lasted for 20 s per time and was repeated 50 times under the same velocity (100 mm min^{-1}) and normal force (2 N). Specifically, 50 data samples of each material are obtained for training (80%) and testing (20%). As shown in Fig. 5b and Supplementary Fig. 6, the corresponding electrical signals reveal different waveforms when sliding on different materials. After the training process by XGBoost, the average discrimination accuracy for six materials reached 93.3%, as depicted in the confusion matrix of Fig. 5c. In addition, for roughness discrimination, six silicon wafers with different roughnesses were prepared through wafer etching into microgrooves with different widths and the same depths ($40 \mu\text{m}$), as shown in Fig. 5d. Under the same velocity of 100 mm min^{-1} and normal force of 2 N, sliding was also repeated 50 times for each roughness, and the resulting details of resistance are shown in Fig. 5e and Supplementary Fig. 7. According to the database and the XGBoost algorithm, the average accuracy for roughness discrimination can reach 92.8%, as depicted in the confusion matrix of Fig. 5f.

Combining the above abilities of material classification and roughness discrimination, we have demonstrated the feasibility of our multifunctional tactile sensor system to recognize the common objects used in daily life, including masks, bananas, oranges, glass, desks and leaves (Fig. 6a). As a proof-of-concept application for HMIs, a person who wears the inspired sensor on the fingertip can estimate objects through dragging on the target surface. First, the

electrical signals were measured by a PCB with a sampling frequency of 100 Hz. Each sliding last 2 s and repeated. Then, the XGBoost classifier was trained with the obtained database. Considering the training efficiency, we compared the average accuracy of different times of repetition, as shown in Supplementary Fig. 8, and chose 50 repetitions with 90.1% average accuracy, as depicted in the confusion matrix of Fig. 6b. Finally, the actual online recognition is shown in Supplementary Movie 4, demonstrating the notable ability for object classification with the multifunction tactile system, which has promising prospects in HMIs.

DISCUSSION

Multifunctional tactile sensing, especially sliding, is an important but neglected way for HMIs to interact with the environment. Relying on sliding, the HMI system can obtain abundant information, such as roughness, material and movement, which is difficult to determine exactly by previous pressure sensors. In summary, based on the theory of the stick-slip phenomenon, we have developed a machine-learning-assisted multifunction tactile system, providing the ability of force sensing, slippage detection, material classification and roughness discrimination.

Imitating the fingertips of humans, we propose a kind of fingertip-inspired tactile sensor structure. The sensor consists of two layers: the epidermis-inspired top layer contains electrodes and microspirals, and the spinous-inspired bottom layer contains micropylamids with SWCNTs. For the multifunction sensing mechanism, force sensing is modulated by the contact resistance, slippage detection is based on the presence of stick-slip phenomena, and material classification and roughness discrimination rely on the characteristics of stick-slip phenomena. By incorporating machine learning into the system, we achieved high standards in terms of recognition rate for slippage detection (100.0%), material classification (93.3%) and roughness discrimination (92.8%). Compared with other technologies developed for object classification, the sensing mechanism of our system offers an innovative approach to estimate material characteristics.

We also set proof-of-concept applications for HMIs. In closed-loop sensing control of robotic hands, robotic fingers equipped with a multifunction sensing system have the ability to detect force and slippage and then work out corresponding actions to achieve feedback control. To improve the enjoyment of HMIs, a Super Mario game was also designed to interact with humans, controlled by hand actions. In addition, the discrimination of six common objects in daily life is shown in Fig. 6. The above proof-of-concept applications indicated that the multifunction sensing system has broad application prospects in HMI.

Our machine-learning-assisted multifunction sensing system improves the ability to activate sensing, but it still has limitations that need to be addressed. Compared with other advanced technologies developed for objects classification, a high-density sensor array is needed to sensing the shape of object in future designs. And in applications of HMI based on our multifunction sensing system, the algorithm model was developed on the server for classification. Implementing efficient machine-learning (ML) algorithms at edge devices for on-site decision-making could be important to further enhance the independence and reduce the power consumption of the system in the future. In addition, for dexterous robotic hands, closed-loop control for slippage of our system is still not as perfect as sensory feedback from humans, especially in the latency of sensing slippage. Further research efforts could also be committed to optimizing the stick-slip theory to achieve slippage prediction. We envision that the machine-learning-assisted multifunction sensing system based on tribology theory could enrich HMI information, especially regarding slippage.

METHODS

Fabrication of epidermis-inspired layer

The fingertip-inspired sensor consists of an epidermis-inspired layer and a spinous-inspired layer. For the fabrication of the epidermis-inspired layer, a silicon mold with spiral microgrooves was prepared by traditional lithography and dry etching processes. The diluted polyimide solution was spin-coated on the cleaned silicon mold and cured at 300 °C for 1 h. After this replicating process, a polyimide film with a double spiral structure can be obtained. Then, interdigital electrodes were printed on the back of the spiral structure by screen printing technology using conductive silver paste.

Fabrication of spinous-inspired layer

For the fabrication of the spinous-inspired layer, a micropylamid mold was prepared first. After conventional photolithography, the silicon wafer was immersed in a 40% wt KOH solution for 10 min at 85 °C to anisotropically etch silicon. Next, SWCNTs were dispersed in N,N-dimethylformamide (DMF) at a concentration of 0.05 mg mL⁻¹ and sprayed on the above silicon mold. Then, the dilute polyimide solution was spin-coated on this mold to obtain SWCNT/PI thin films. Finally, the fingertip-inspired sensor was assembled by pasting the epidermis-inspired layer and spinous-inspired layer together with adhesive tape on the edge.

Device characterization

Resistance measurements were taken using a Keithley 2602 or PCB, as depicted in Supplementary Fig. 1. Normal force sensing ability was tested by a customized apparatus, which contains a force gauge and an X-axis electric moving stage (Beijing Optical Century Instrument Co., LTD., SC100 series stepper motor controllers). Sliding movement was set up by the MXD-02 friction coefficient apparatus (Labthink Instruments Co., Ltd., Jinan, China).

Circuit design

As shown in Supplementary Fig. 1, the resistance of the fingertip-inspired sensor was measured by voltage division. A microprocessor unit (MPU) was used to process the original signal and then convert the analogue signals to digital signals. A voltage regulator chip provides a stable power supply for the whole circuit. With the USB-TTL module, the resistance value of the sensor can be read on the terminal in real time.

The statement for human subjects

All authors, Yue Li, Tie Li, and Ting Zhang, have obtained a disclaimer of signed informed consent from the person who participated in our sensor testing experiments in Figs. 3, 4, 6 with human subjects.

DATA AVAILABILITY

The original datasets that support the plots within this paper are available from the corresponding authors upon reasonable request.

CODE AVAILABILITY

The codes that support the findings within this paper are available from the corresponding authors upon reasonable request.

Received: 11 February 2022; Accepted: 30 May 2022;

Published online: 17 June 2022

REFERENCES

- Li, G., Liu, S., Wang, L. & Zhu, R. Skin-inspired quadruple tactile sensors integrated on a robot hand enable object recognition. *Sci. Robot.* **5**, eabc8134 (2020).
- Sundaram, S. How to improve robotic touch Challenges for instrumenting robotic hands to match human performance are outlined. *Science* **370**, 768–769 (2020).
- Kim, T. et al. Heterogeneous sensing in a multifunctional soft sensor for human-robot interfaces. *Sci. Robot.* **5**, eabc6878 (2020).
- Khan, M., Silva, B. N. & Han, K. Internet of things based energy aware smart home control system. *IEEE Access* **4**, 7556–7566 (2016).
- Li, M. & Lin, H. J. Design and implementation of smart home control systems based on wireless sensor networks and power line communications. *IEEE Trans. Ind. Electron.* **62**, 4430–4442 (2015).

6. Yu, X. et al. Skin-integrated wireless haptic interfaces for virtual and augmented reality. *Nature* **575**, 473–479 (2019).
7. Zhu, M. et al. Haptic-feedback smart glove as a creative human-machine interface (HMI) for virtual/augmented reality applications. *Sci. Adv.* **6**, eaaz8693 (2020).
8. Zhou, Z. et al. Sign-to-speech translation using machine-learning-assisted stretchable sensor arrays. *Nat. Electron.* **3**, 571–578 (2020).
9. D'Anna, E. et al. A closed-loop hand prosthesis with simultaneous intraneural tactile and position feedback. *Sci. Robot.* **4**, eaau8892 (2019).
10. Dong, B. et al. Wearable triboelectric-human-machine interface (THMI) using robust nanophotonic readout. *ACS Nano* **14**, 8915–8930 (2020).
11. Muthukumarana, S., Elvitigala, D. S., Forero Cortes, J. P., Matthies, D. J. & Nanayakkara, S. Touch me gently: recreating the perception of touch using a shape-memory alloy matrix. *Proceedings of the 2020 CHI Conference on Human Factors in Computing Systems*, New York, NY: Association for Computing Machinery, 1–12. <https://doi.org/10.1145/3313831.3376491> (2020).
12. Araromi, O. A. et al. Ultra-sensitive and resilient compliant strain gauges for soft machines. *Nature* **587**, 219–224 (2020).
13. Yang, Y. et al. A non-printed integrated-circuit textile for wireless theranostics. *Nat. Commun.* **12**, 4876 (2021).
14. Shi, J. et al. Smart textile-integrated microelectronic systems for wearable applications. *Adv. Mater.* **32**, 1901958 (2019).
15. Yao, H. et al. Near-hysteresis-free soft tactile electronic skins for wearables and reliable machine learning. *Proc. Natl Acad. Sci. U.S.A.* **117**, 25352–25359 (2020).
16. Lee, J. H. et al. A behavior-learned cross-reactive sensor matrix for intelligent skin perception. *Adv. Mater.* **32**, e2000969 (2020).
17. Jiang, C. et al. A high-performance bionic pressure memory device based on piezo-OLED and piezo-memristor as luminescence-fish neuromorphic tactile system. *Nano Energy* **77**, 105120 (2020).
18. Chen, Y. et al. Piezotronic graphene artificial sensory synapse. *Adv. Funct. Mater.* **29**, 1900959 (2019).
19. Boutry, C. M. et al. A hierarchically patterned, bioinspired e-skin able to detect the direction of applied pressure for robotics. *Sci. Robot.* **3**, eaau6914 (2018).
20. Viry, L. et al. Flexible three-axial force sensor for soft and highly sensitive artificial touch. *Adv. Mater.* **26**, 2659–2664 (2014).
21. Chen, H. et al. Fingertip-inspired electronic skin based on triboelectric sliding sensing and porous piezoresistive pressure detection. *Nano Energy* **40**, 65–72 (2017).
22. Wang, Y. et al. Hierarchically patterned self-powered sensors for multifunctional tactile sensing. *Sci. Adv.* **6**, eabb9083 (2020).
23. Charalambides, A. & Bergbreiter, S. Rapid manufacturing of mechanoreceptive skins for slip detection in robotic grasping. *Adv. Mater. Technol.* **2**, 1600188 (2017).
24. Ren, Z. et al. Fully elastic and metal-free tactile sensors for detecting both normal and tangential forces based on triboelectric nanogenerators. *Adv. Funct. Mater.* **28**, 1802989 (2018).
25. Yamaguchi, T., Kashiwagi, T., Arie, T., Akita, S. & Takei, K. Human-like electronic skin-integrated soft robotic hand. *Adv. Intell. Syst.* **1**, 1900018 (2019).
26. Schwarz, C. The slip hypothesis: tactile perception and its neuronal bases. *Trends Neurosci.* **39**, 449–462 (2016).
27. Weber, A. I. et al. Spatial and temporal codes mediate the tactile perception of natural textures. *Proc. Natl Acad. Sci. U.S.A.* **110**, 17107–17112 (2013).
28. Johansson, R. S. & Flanagan, J. R. Coding and use of tactile signals from the fingertips in object manipulation tasks. *Nat. Rev. Neurosci.* **10**, 345–359 (2009).
29. Thompson, P. A. & Robbins, M. O. Origin of stick-slip motion in boundary lubrication. *Science* **250**, 792–794 (1990).
30. Berman, A. D., Ducker, W. A. & Israelachvili, J. N. Origin and characterization of different stick-slip friction mechanisms. *Langmuir* **12**, 4559–4563 (1996).
31. Heslot, F., Baumberger, T., Perrin, B., Caroli, B. & Caroli, C. Creep, stick-slip, and dry-friction dynamics: experiments and a heuristic model. *Phys. Rev. E* **49**, 4973–4988 (1994).
32. Popov, V. L. *Contact mechanics and friction: physical principles and applications* (Springer Science & Business Media, 2010).
33. Ponomarev, I. V. & Meyerovich, A. E. Surface roughness and effective stick-slip motion. *Phys. Rev. E* **67**, 026302 (2003).
34. Oden, J. T. & Martins, J. Models and computational methods for dynamic friction phenomena. *Comput. Methods Appl. Mech. Eng.* **52**, 527–634 (1985).
35. Delhay, B., Lefevre, P. & Thonnard, J. L. Dynamics of fingertip contact during the onset of tangential slip. *J. R. Soc. Interface* **11**, 20140698 (2014).
36. Andre, T., Levesque, V., Hayward, V., Lefevre, P. & Thonnard, J. L. Effect of skin hydration on the dynamics of fingertip gripping contact. *J. R. Soc. Interface* **8**, 1574–1583 (2011).
37. Tada, M. & Kanade, T. An imaging system of incipient slip for modelling how human perceives slip of a fingertip. *26th Annu. Int. Conf. IEEE Eng. Med. Biol. Soc.* **1**, 2045–2048 (2004).
38. Bensmaïa, S. J. & Hollins, M. The vibrations of texture. *Somatosens. Mot. Res.* **20**, 33–43 (2003).
39. Scheibert, J., Leurent, S., Prevost, A. & Debrégeas, G. The role of fingerprints in the coding of tactile information probed with a biomimetic sensor. *Science* **323**, 1503–1506 (2009).
40. Abaira, V. E. & Ginty, D. D. The sensory neurons of touch. *Neuron* **79**, 618–639 (2013).

ACKNOWLEDGEMENTS

The authors acknowledge the funding support from the National Key R&D Program of China (2017YFA0701101, 2018YFB1304700, 2020YFB2008501), the National Science Fund for Distinguished Young Scholars of China (62125112), the National Natural Science Foundation of China (62071462, 62071463), the Youth Promotion Association of Chinese Academy of Sciences (2020320), the Foundation Research Project of Jiangsu Province (BK20201195, BK20200259) and the Zhejiang Lab's International Talent Fund for Young Professionals (ZJ2020GZ016); the Suzhou Key Industrial Technology Innovation Project (SYG202029). The authors are grateful for the technical support from Nano-X Vacuum Interconnected Workstation of Suzhou Institute of Nano-Tech and Nano-Bionics, Chinese Academy of Sciences (SINANO).

AUTHOR CONTRIBUTIONS

Y.L., T.L., and T.Z. conceived the idea and designed the experiments. Y.L. and Z.X. designed and optimized the sensor. M.Z., and L.H. contribute to the software and PCB circuit board with help from Y.D. and Y.W. Y.L., M.Z., and L.H. performed subject studies with assistance from Y.W. T.L., and T.Z. supervised the work and edited the paper. All authors discussed the results and commented on the paper at all stages. All authors are in agreement with the content of paper.

COMPETING INTERESTS

The authors declare no competing interests.

ADDITIONAL INFORMATION

Supplementary information The online version contains supplementary material available at <https://doi.org/10.1038/s41528-022-00183-7>.

Correspondence and requests for materials should be addressed to Tie Li or Ting Zhang.

Reprints and permission information is available at <http://www.nature.com/reprints>

Publisher's note Springer Nature remains neutral with regard to jurisdictional claims in published maps and institutional affiliations.



Open Access This article is licensed under a Creative Commons Attribution 4.0 International License, which permits use, sharing, adaptation, distribution and reproduction in any medium or format, as long as you give appropriate credit to the original author(s) and the source, provide a link to the Creative Commons license, and indicate if changes were made. The images or other third party material in this article are included in the article's Creative Commons license, unless indicated otherwise in a credit line to the material. If material is not included in the article's Creative Commons license and your intended use is not permitted by statutory regulation or exceeds the permitted use, you will need to obtain permission directly from the copyright holder. To view a copy of this license, visit <http://creativecommons.org/licenses/by/4.0/>.

© The Author(s) 2022